The Pathologic Role of Intracellular *Cutibacterium acnes* in Intractable Oral Inflammation

Han, Dawool

Department of Dentistry

Graduate School

Yonsei University

The Pathologic Role of Intracellular *Cutibacterium acnes* in Intractable Oral Inflammation

Advisor Professor Kim, Hyun Sil

A Dissertation Submitted
to the Department of Dentistry
and the Committee on Graduate School
of Yonsei University in Partial Fulfillment of the
Requirements for the Degree of
Doctor of Philosophy in Dental Science

Han, Dawool

June 2025

The Pathologic Role of Intracellular *Cutibacterium acnes* in Intractable Oral Inflammation

This Certifies that the Dissertation of Han, Dawool is Approved

Committee Chair	**Yook, Jong In**
Committee Member	**Kim, Hyun Sil**
Committee Member	**Lee, Jung Seok**
Committee Member	**Cho, Eunae Sandra**
Committee Member	**Kim, Nam Hee**

Department of Dentistry
Graduate School
Yonsei University
June 2025

감사의 글

박사학위 논문을 마무리하며, 지금까지의 여정에 함께해주신 모든 분들께 깊은 감사의 마음을 전합니다.

먼저, 부족한 저를 끊임없이 지도해주시고 연구자로서의 자세와 방향을 가르쳐주신 육종인, 김현실, 조은애산드라, 김남희 교수님께 진심으로 감사드립니다. 교수님의 따듯한 격려와 조언은 제 학문적 성장의 가장 큰 밑거름이 되었습니다. 항상 구강병리학자로서 기준을 잃지 않도록 이끌어 주셔서 지금의 제가 있을 수 있었습니다.

또한, 공동연구를 통해 많은 배움과 도움을 주신 이중석 교수님 그리고 김도현 교수님께 감사의 말씀을 드립니다. 처음 다뤄보는 미생물학적 실험에 자문을 드릴때마다 늘 도움을 주시고 아낌없는 지원을 해주시고 미생물학교실 신성재 교수님께도 진심으로 감사드립니다.

연구실의 선후배 및 동료 연구원 선생님들께도 깊이 감사드립니다. 이름을 일일이 나열하지는 못하지만, 함께한 모든 분들과의 소중한 인연이 저에게는 큰 배움이자 힘이었습니다. 실험실에서 함께 고민하고 토론하고 해결해 나가는 과정이 없었다면 이 연구는 완성될 수 없었을 것입니다. 평상시에 표현하지 못한 감사의 마음을 이제야 전합니다.

늘 곁에서 묵묵히 응원해주시고 믿어주신 사랑하는 부모님과 가족에게 가장 큰 감사를 전합니다. 어려운 시기마다 보내주신 믿음과 격려, 사랑이 있었기에 어려운 길 포기하지 않고 도전할 수 있었습니다.

마지막으로, 이 연구가 과학적으로나 임상적으로 작은 기여라도 될 수 있기를 소망하며, 함께 해주신 모든 분들께 다시 한 번 진심으로 감사드립니다.

2025년 6월
한다울 올림

TABLE OF CONTENTS

LIST OF FIGURES

LIST OF TABLES

ABSTRACT

The Pathologic Role of Intracellular *Cutibacterium acnes* in Intractable Oral Inflammation

Cutibacterium acnes (C. acnes), a Gram-positive anaerobic commensal bacterium of the skin and mucosa, has recently emerged as potential pathogen in various chronic inflammatory diseases. Notably, its ability to persist intracellularly within macrophages suggests a mechanism of immune evasion and chronic inflammation. However, the role of intracellular *C. acnes* in chronic oral inflammatory diseases remains poorly understood. In this study, intracellular *C. acnes* strains were isolated from the lesions of the peri-implantitis and apical periodontitis and their characteristics of intracellular pathogen were investigated using both in vitro and in vivo models.

The isolated strains survived within Raw 264.7 macrophages for several days without being degraded, as confirmed by immunofluorescence imaging and recovery from anaerobic bacterial culture. Although intracellular proliferation was not evident, transmission to neighboring uninfected macrophages was observed, indicating intercellular spreading capacity. These findings support the hypothesis that *C. acnes* can persist within host cells and disseminate through macrophage populations.

C. acnes infection triggered robust pro-inflammatory responses in macrophages. RT-qPCR and cytokine array revealed significant upregulation of key inflammatory cytokines and chemokines, including IL-6, CCL2 and CSF. Bulk RNA sequencing further identified 1,672 upregulated and 1,464 downregulated genes associated with microbial infection, cytokine signaling, and microbial recognition pathways. In vivo, subcutaneously injected *C. acnes* was detected within $CD68^+$ macrophages in mouse tissues, accompanied by granulomatous inflammation and elevated expression of IL-1β, IL-23, and TNF-α.

These findings suggest that *C. acnes* acts as a persistent intracellular pathogen in chronic oral inflammatory diseases, capable of resisting degradation, inducing pro-inflammatory cytokines, and contributing to granuloma formation. This mechanism may underlie therapeutic resistance and highlights the need for intracellular-targeted treatment strategies in intractable oral inflammation.

Key words: Cutibacterium acnes, Macrophages, Intracellular Pathogen, Inflammation, Infection, Peri-implantitis, Apical Periodontitis, Intractable Oral Inflammation

1. Introduction

Cutibacterium acnes (C. acnes) is a gram positive, aerotolerant anaerobic bacterium that constitutes a major part of the commensal microbiota of the skin and mucous membrane. Although historically studied as the causative pathogen of acne vulgaris, recent evidence suggests its potential involvement in a wide range of chronic inflammatory conditions (Mayslich et al., 2021). *C. acnes* is frequently isolated from prosthetic joint infection and post-surgical infection, and notably, it is the only cultivable microorganism consistently recovered from sarcoidosis lesions (Eishi, 2013; Eishi, 2023; Negi et al., 2012). Additionally, *C. acnes* infection has been implicated in unexpected conditions such as prostatitis, prostate cancer, and intervertebral disc disease (Ashida et al., 2024; Bae et al., 2014; Capoor et al., 2021; Davidsson et al., 2021).

A key characteristic of *C. acnes* which has garnered increasing scientific attention is its ability to persist intracellularly within macrophages. Intracellular pathogens are capable of evading host immune defense and persisting within phagocytes. Unlike typical bacteria that are cleared via phagolysosomal degradation, intracellular pathogens developed mechanisms to avoid this fate. For instance, *Mycobacterium tuberculosis* prevents phagolysosome formation, while *Listeria monocytogenes* escapes from the phagosome into the cytosol (Thakur et al., 2019). These intracellular pathogens can use macrophages as reservoirs, replicating intracellularly and spreading to adjacent host cells, may triggering granulomatous inflammation. In sarcoidosis, the fact that *C. acnes* is the only cultivable microorganism supports its role as a putative intracellular pathogen (Eishi, 2013). Several researches by Eishi and colleagues demonstrates that *C. acnes* resides within alveolar macrophages and perihilar lymph nodes in sarcoidosis and exhibits microscopical features consistent with both intracellular proliferation and latent infection (Eishi, 2013; Eishi, 2023; Negi et al., 2012). Also, they proved intratracheal injection of *C. acnes* can induce pulmonary granuloma in mice model (Nishiwaki et al., 2004; Werner et al., 2017).

The oral cavity harbors a highly diverse microorganisms comprising 700 to 1500 species, and perturbations in the microbiota have been linked to chronic inflammatory conditions (Deo & Deshmukh, 2019). Although *C. acnes* infection in oral inflammatory diseases is less well characterized, several studies have identified its presence in some microbiome researches in oral inflammatory diseases (Niazi et al., 2016; Persson & Renvert, 2014; Tamura et al., 2013; Wallis et

al., 2011). In my previous study, I identified intracellular *C. acnes* in idiopathic granulomatous lesions of the chin and peri-oral skin, in associated with endo-periodontal lesions (Han et al., 2024). Moreover, we demonstrated the presence of intracellular *C. acnes* within macrophages in peri-implantitis tissues using PCR (polymerase chain reaction) test and immunohistochemical staining using PAB antibody (Park et al., 2024).

In this study, I aimed to investigate pathogenic mechanism of *C. acnes* as an intracellular bacterium in intractable oral inflammatory diseases. I isolated intracellular *C. acnes* from apical periodontitis and periodontitis, and examined its persistence, intracellular proliferation, and intercellular propagation. Furthermore, I utilized an in vivo murine model to prove whether intracellular *C. acnes* infection can induce granulomatous inflammation. Based on these finding it might be helpful to develop novel therapeutic strategies targeting intracellular *C. acnes* in refractory oral inflammatory diseases.

2. Materials and Methods

2.1. Isolation of Intracellular *C. acnes* in intractable oral inflammatory diseases

Tissue sample were obtained from patients diagnosed with peri-implantitis and apical periodontitis at Yonsei University Dental Hospital and immediately transferred to the laboratory. After PBS washing, the tissues were minced using sterile scissors and incubated in 1 mg/mL type I collagenase (Gibco, #17100017) at 37°C with gently shaking. Following first dissociation through a 70μm cell strainer, red blood cells were lysed using ACK lysing buffer (Gibco, #A1049201). Final single cell suspension was prepared using 40μm cell strainer. $CD14^+$ and $CD14^-$ cell populations were separated by magnetic-activated cell sorting (MACS; Miltenyi Biotec, #130-050-201). Sorted cells were cultured in DMEM supplemented with high concentrations of antibiotics (penicillin 200U/mL, streptomycin 200μg/mL, amphotericin B 0.5μg/mL, Gibco, #15240-062) for 24 hours to eliminate extracellular bacteria. After a day of incubation, cells were lysed with 0.05% Triton X-100 lysis buffer, and lysates were plated on blood agar plates and incubated anaerobically for more than two weeks.

Colonies that grew under anaerobic condition were suspended in distilled water and subjected to PCR (Polymerase Chain Reaction) test targeting the *C. acnes* 16S rRNA gene and roxP gene. The primer sequences for the PCR test used in this study are listed in Table 1. Colonies positive for *C. acnes*-specific gene were further confirmed by Sanger Sequencing. Verified *C. acnes* isolates were cultured in thioglycolate broth and stored in 20% glycerol at -80°C for subsequent use.

The study was conducted according to the guidelines of the Declaration of Helsinki, and approved by the Institutional Review Board (or Ethics Committee) of Yonsei University Health System, Seoul, Republic of Korea (IRB No. 2-2022-0036)

Table1. Primer sequence for PCR test to identify *C. acnes*

Gene name	Forward (5’ -> 3’)	Reverse (5’ -> 3’)
16s rRNA	GGGTTGTAAACCGCTTTCGCCT	TTCGACGGCTCCCCCACAAC

roxP	CGTCAATTCCCATACGTACGA	CACCATGAATGTCTTGACGCT

2.2. Bacterial Culture

Cutibacterium acnes strains were maintained in thioglycolate broth and sub-cultured every two weeks by transferring a 1:20 dilution into fresh medium. For experimental use, bacteria were transferred at a 1:20 ratio into fresh brain-heart-infusion (BHI) broth and cultured anaerobically for 47-72 hours. Anaerobic condition was established using the BD GasPakTM EZ container system (BD, #260678). Heat-killed *C. acnes* was prepared by incubating the same amount of *C. acnes* D1 strain in a 70°C water bath for 30 minutes.

In addition to the D1 and D2 strains isolated in this study, three additional C. acnes strains-KBN12P07016, KBN12P05481, KBN12P07215)-were provided by Gyeongsang National University Hospital Branch of the National Culture Collection for Pathogen (GNUH-NCCP). Furthermore, the *C. acnes* C1 strain, originally isolated from a cutaneous sarcoidosis patient (Minegishi et al., 2015), was generously provided by Professor Yoshinobu Eishi from Tokyo Medical and Dental University, Tokyo, Japan.

2.3. Infection of macrophage cell lines with *C. acnes*

THP-1 and Raw264.7 Cells were seeded at 30% confluency in 6-well plates and incubated for 24 hours. THP-1 cells were cultured in RPMI 1640, and Raw 264.7 cells in DMEM, each supplemented with 10% fetal bovine serum (FBS; Gibco, #16000044) and 1% penicillin/streptomycin/fungizone (P/S/F). Prior to infection, cells were washed, and the media changed with antibiotics-free medium. *C. acnes* D1 or D2 strains were added at the desired multiplicity of infection (MOI), while the control group received an equal volume of BHI broth. After 24 hours of infection, cells were washed three times with PBS and incubated for additional 4 hours in medium containing high amounts of gentamycin (200μg/mL, Sigma-Aldrich, #345814) to eliminate extracellular bacteria. Cells were then cultured for the desired post-infection time period, with the media changed every 24 hours.

2.4. Production of rabbit polyclonal antibody against *C. acnes*

10-week-old rabbits were acclimatized prior to immunization. For initial immunization, live *C. acnes* D1 strain ($2x10^9$ CFU) was injected subcutaneously in the flank. Four weeks after the initial injection, booster doses containing $1x10^9$ CFU of *C. acnes* D1 were administrated at 2-week intervals, for a total of four booster injections. Whole blood was collected in the SST (serum separating tube) and centrifuged at 3,000 rpm for 10minutes to separate serum. The polyclonal antibody was purified from serum using a Protein A column affinity purification system. This antibody against *C. acnes* was designated anti-CA antibody.

2.5. Proliferation assay of intracellular *C. acnes*

Raw 264.7 cells were seeded at 30% confluency onto 4 well chamber slides. Cells were infected with live *C. acnes* D1 or D2 strains, or heat-killed *C. acnes*, at a MOI of 15. At designated time points (24, 48, and 72 hours post-infection), cell were fixed with 4% paraformaldehyde and subjected to immunofluorescence staining using PAB antibody to detect intracellular *C. acnes*. Images were acquired from five randomly selected fields per condition. The intracellular *C. acnes* burden was quantified using ImageJ by measuring the signal intensity in the green (PAB) and blue (DAPI) channel. The PAB signal was normalized to the DAPI signal to estimate the average *C. acnes* burden per cell.

2.6. Detection of intercellular spreading of intracellular *C. acnes*

To visualize intercellular transfer of intracellular *C. acnes*, a stable Raw 264.7 cell line expressing red fluorescence protein (dsRED) was generated using a lentiviral vector system. Wild-type Raw 264.7 cells (not expressing dsRED) were infected with *C. acnes* D1 or D2 strains at a multiplicity of infection (MOI) of 100. After 24 hours of infection, extracellular bacteria were eliminated by treating with 200 μg/mL gentamicin for 4 hours. Infected wild-type Raw 264.7 cells were then mixed with uninfected Raw 264.7-dsRED cells at 1:9 ratio and co-cultured for 5 days. At the end of the co-cultured period, cells were fixed and stained with PAB antibody for detection of *C. acnes*, followed by immunofluorescence imaging using confocal microscopy. The presence of *C.*

acnes in dsRED-positive cells was assessed to evaluate potential cell-to-cell transmission.

2.7. Proliferation and viability assay of *C. acnes*-infected Raw 264.7 cells

To evaluate the impact of *C. acnes* infection on macrophage proliferation, Raw 264.7 cells were infected with the *C. acnes* D1 strain at a multiplicity of infection (MOI) of 100. Viable cell numbers were assessed over time using trypan blue exclusion assay. Only trypan blue-negative (viable) cells were counted.

To assess cytotoxicity associated with *C. acnes* infection, Raw 264.7 cells were exposed to varying MOIs of C. acnes D1 strain (0, 10, 20, 50, and 100). After 24 hours of infection, extracellular bacteria were removed using gentamycin treatment. Cell were then transferred to a 96-well plate and incubated for an additional 24 hours. Cell viability was evaluated using the MTT [3-(4,5-dimethylthiazol-2-yl)-2,5-diphenyltetrazolium bromide] assay.

2.8. Reverse Transcription Quantitative PCR (RT-PCR)

Raw 264.7 cells were infected with *C. acnes* D1 and D2 strains at a multiplicity of infection (MOI) of 100. After 24 hours, total RNA was extracted using TRIzol reagent (Invitrogen, #15596018). Complementary DNA (cDNA) was synthesized using random hexamer primer (dN6) with the AccuPower® CycleScript RT Premix (Bioneer, #K2044). Quantitative PCR was performed using the 7300 Real-Time PCR system (Applied Biosystem) and TB Green® Premix Ex Taq™ II (Takara). Gene expression was calculated using the ΔCT method and normalized to the housekeeping gene eEF-2. The primer sequences used in this study are listed in Table 2.

Table 2. Primer Sequence for RT-qPCR

Gene name	Forward (5' -> 3')	Reverse (5' -> 3')
eEF2	CGTCAATTCCCATACGTACGA	CACCATGAATGTCTTGACGCT
IL-1α	ACGGCTGAGTTTCAGTGAGACC	CACTCTGGTAGGTGTAAGGTGC

IL-1β	TGGACCTTCCAGGATGAGGACA	GTTCATCTCGGAGCCTGTAGTG
IL-6	TACCACTTCACAAGTCGGAGGC	CTGCAAGTGCATCATCGTTGTTC
IL-23	CCCCTTCTCCGTTCCAAGAT	AACCTGGGCATCCTTAAGCT
TNF-α	TGAGGTCAATCTGCCCAAGT	GGGGTCAGAGTAAAGGGGTC
CCL2	CAGCTCTCTCTTCCTCCACC	TGGGATCATCTTGCTGGTGA
CSF2	CTGCGTAATGAGCCAGGAAC	TCTCTCGTTTGTCTTCCGCT
TGF-β	AGAGACGTGGGGACTTCTTG	GAATAGGGGCGTCTGAGGAA

2.9. Cytokine Array

Culture supernatants were collected 24 hours after infection of Raw 264.7 cells with *C. acnes* D1 and D2 strains (100 MOI). During the final incubation period, cells were maintained in DMEM containing 0.1% BSA without FBS. A total of 1.5mL of conditioned media was used for analysis with the Mouse Inflammation Array C1 Kit (RayBiotech, #AAM-INF-1-8) according to the manufacturer's protocol. Briefly, membrane-based cytokine arrays were pre-blocked and incubated with the sample 16 hours at 4°C. After washing, membranes were sequentially incubated with a biotin-conjugated antibody cocktail and HRP-conjugated streptavidin. Signal detection was performed using enhanced chemiluminescence (ECL) reagents provided in the kit, and membranes were exposed to X-ray film (AGFA, #AGFA810) for signal visualization. Dot intensities were subsequently quantified by ImageJ program. The intensity of signals was normalized with positive control signal.

2.10. Transcriptome analysis (bulk RNA sequencing)

To evaluate the transcriptional response of macrophages to *C. acnes* infection, Raw 264.7 cells were infected with six *C. acnes* strains (including D1 and D2; see section 2.2) at a multiplicity of infection (MOI) of 100. After 24 hours, total RNA was extracted from each group. Control group was treated with an equal volume of BHI medium. RNA sequencing was performed using the

Illumina HiSeq2500 platform. Differentially expressed gene (DEGs) were identified using the edgeR package, analysing 21,970 protein-coding genes. Genes with a |log fold change (logFC)| > 1 and a false discovery rate (FDR) < 0.05 were considered significant. Based on these results, volcano plot and KEGG pathway analyses were generated for further interpretation.

Transcriptomic comparisons were carried out between the following groups

- All *C. acnes*-infected group vs Control group
- Intracellular *C. acnes* strains (C1, D1, D2 strain) vs Extracellular *C. acnes* strains (KBN12P07016, KBN12P05481, KBN12P07215)

Transcription factor activity inference was performed using CollecTRI gene regulatory network scoring with the Python package decoupler (v2.0.7) on the bulk RNA-seq dataset (Phyoton 3.10.17). Activity scores were used to rank TFs based on enrichment of their downstream target genes between infected and control conditions.

2.11. Subcutaneous injection of *C. acnes* in mice

Seven-week-old male C57bl/6 mice were used for subcutaneous injection experiments following a one-week acclimation period. The dorsal skin was shaved using a trimmer and disinfected with 70% ethanol swabs prior to injection. Live *C. acnes* (D1 or D2 strain) and heat-killed *C. acnes* were suspended in a hyaluronic acid and PBS mixture (6:4 ratio) to enhance local retention. A total of $1x10^8$ CFU in 100 μL volume was injected subcutaneously into both sides of the dorsal regions. Mice received two injections at the same sites at 7-day interval and were euthanized 7 days after the final injection. The study scheme was approved by the Institutional Animal Care and Use Committee (IACUC) of Yonsei University College of Medicine (IACUC number: 2024-0145).

Skin tissues from the injection sites, including dermis to the depth of skeletal muscle tissue or peritoneum, were harvested and immediately fixed in 10% neutral buffered formalin for 24 hours. Fixed tissues were processed for paraffin embedding (FFPE) and sectioned for histological and immunohistochemical analysis.

Hematoxylin and eosin (H&E) staining was performed on tissue section to evaluate inflammation. Inflammation was scored based on following criteria.

0: No inflammation

1: Inflammatory cells infiltration without organized structure

2: Collection of inflammatory cells including macrophages, indicative of granuloma formation

3: Granuloma formation with central necrosis

For each mouse, the highest score from both injection sites was recorded, and the average of the two was used to determine the inflammation score per animal

Immunohistochemical analysis was conducted to detect bacterial and immune markers. For quantification, five random field per sample were imaged under identical exposure setting. DAB and hematoxylin signals were separated using ImageJ software, and DAB signal intensity was measured to quantify immunoreactivity.

2.12. Transmission Electron Microscopy (TEM)

THP-1 cells after 24 hours of infection at a MOI of 10 were fixed for 24 hours in 2% glutaraldehyde and 2% paraformaldehyde in 0.1M phosphate buffer (pH 7.4), and post-fixed in 1% osmium tetroxide (OsO_4) for 2 hours. Sample were dehydrated through a graded ethanol series (50% to 100%) and infiltrated with propylene oxide for 10 minutes. Cells were embedded in Poly/Bed 812 (Polyscience) and polymerized at 70°C for 12 hours. Semithin section (200nm) were cut using an ultramicrotome (UC7), stained with toluidine blue, and examined under a light microscope. Ultrathin section (80nm) were collected on copper grids, stained with 5% uranyl acetate for 20 minutes and 3% lead citrate for 7 minutes. Imaging was performed using a Hitachi HT7800 transmission electron microscope with a digital camera, operated at an acceleration voltage of 100kV.

2.13. Immunohistochemical (IHC) staining

Immunohistochemical staining was performed as previously described (Park et al., 2024).

Briefly, formalin-fixed, paraffin-embedded tissue sections were deparaffinized and rehydrated, followed by antigen retrieval using citrate buffer (pH 6.0) heated to boiling. Endogenous peroxidase activity was blocked with 3% hydrogen peroxide, and nonspecific binding was blocked using 2.5% normal goat serum. Primary antibodies were applied and incubated overnight at 4 °C for 16 hours. The following primary antibodies were used: anti-*C. acnes* polyclonal antibody (PAB, MBL Life Science, #D371-3), custom-made anti-*C. acnes* antibody (Anti-CA antibody), anti-IL-1β (Abcam, #ab9722), anti-CD68 (Agilent, #M0876; Cell Signaling Technology, #97778), anti-IL-23 (Abcam, #ab45420), and anti-TNF-α (Invitrogen, #PA5-19810). Detection and color development were performed using the EnVision Detection System (Agilent, #K5007) according to the manufacturer's protocol.

2.14. Immunofluorescence (IF) staining

Cells cultured in a 4 well chamber slide were fixed with 4% paraformaldehyde and followed by subsequent PBS washing. Permeabilization was carried using 0.5% Triton X-100 in PBS, followed by blocking in 5% normal goat serum in PBS. Primary antibodies were applied and incubated overnight at 4°C. After washing with PBS-T (PBS with 0.1% Tween-20) three times, fluorophore-conjugated secondary antibodies (Invitrogen, Alexa Fluor™ series) were applied at room temperature for 1 hour. After three final washes with PBS-T, slides were mounted with mounting medium containing DAPI (Invitrogen, #8961) and imaged under a confocal microscope (Carl Zeiss, LSM700).

2.15. Statistical Analysis

One-way analysis of variance (ANOVA) with Bonferroni's multiple comparison post hoc test was conducted for data from cell viability test of Raw 264.7 infected by *C acnes*. For all other experiments, the Mann-Whitney test was performed to compare each test group with the control group. Statistical significance was demonstrated as $p < 0.05$ (*), $p < 0.01$ (**), and $p<0.001$ (***). Statistical analysis was conducted using GraphPad Prism 8 (ver. 8.0.2; GraphPad Software, San Diego, CA, USA)

3. Results

3.1. Intracellular infection of *C. acnes* in intractable oral inflammatory diseases

To investigate whether *C. acnes* is present in intractable oral inflammatory diseases, we performed histological and immunohistochemical analyses on tissues obtained from patients diagnosed with peri-implantitis and apical periodontitis. In my previous case series study, the presence of intracellular *C. acnes* in macrophages was confirmed by PCR and immunohistochemistry from extensive peri-implantitis lesions (Park et al., 2024).

In the present study, intracellular *C. acnes* was observed in both peri-implantitis and apical periodontitis specimens. Co-immunostaining for C. acnes and CD68 revealed that the bacteria were localized within CD68-positive macrophages (Figure 1A). Although the inflammatory response was mixed, not granulomatous as in sarcoidosis, macrophages harboring intracellular *C. acnes* were found in areas of mixed inflammation composed of lymphocytes, plasma cells, and neutrophils (Figure 1A).

Moreover, IL-1β expression was diffusely increased throughout the inflammatory tissues, as demonstrated by immunohistochemical staining (Figure 1A). The upregulated IL-1β expression indicates that the lesions were in a pro-inflammatory microenvironment. Together, these findings-intracellular location of *C. acnes* within macrophages and the increased inflammatory milieu-formed the basis of my hypothesis that intracellular persistence of *C. acnes* within macrophages contributes to sustained inflammation and immune evasion, prompting me to investigate its intracellular behavior and pathogenic potential in the present study (Figure 1B).

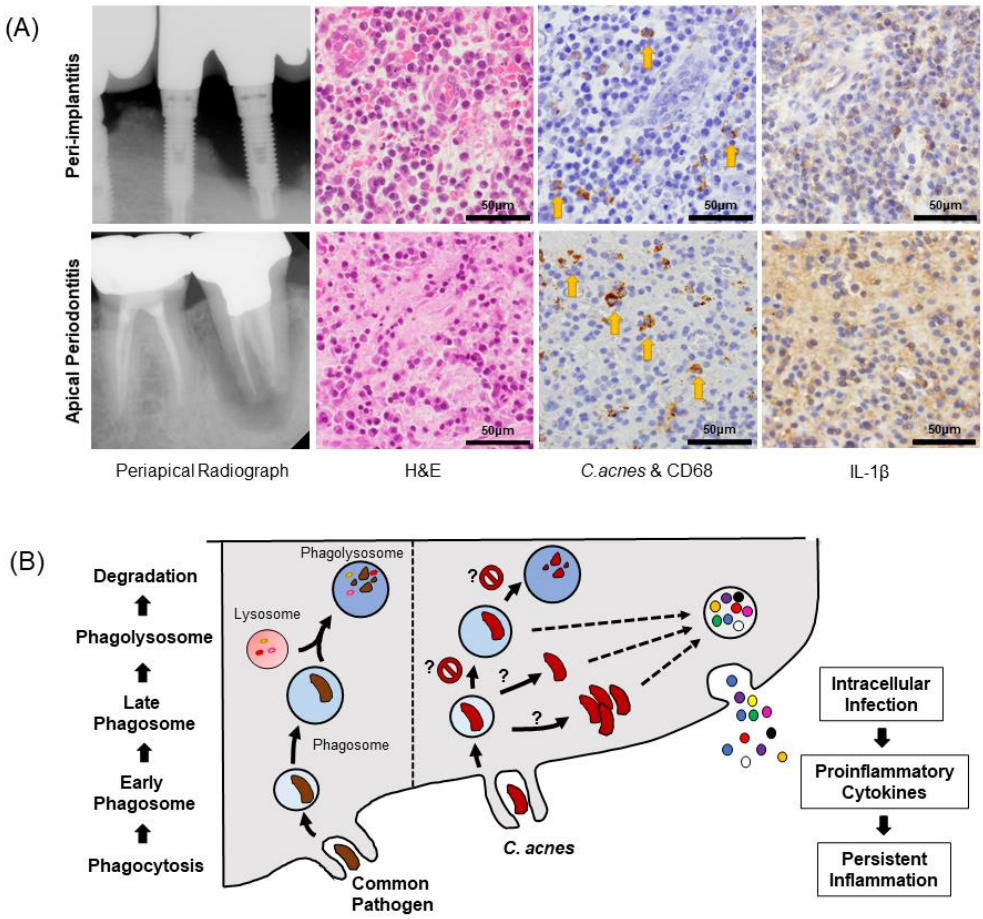

Figure 1. Intracellular infection of *Cutibacterium acnes* in peri-implantitis and apical periodontitis and proposed immunopathogenic model.

(A) Representative clinical and histopathological images from a patient with aggressive peri-implantitis (upper row) and refractory apical periodontitis (lower row). Periapical radiograph shows radiolucent lesions around the implant fixture and at the apex of tooth #37. H&E staining of the surgical tissue reveals swelling and infiltration of various acute and chronic inflammatory cells. Dual immunohistochemical staining was performed using PAB antibody for *C. acnes* (magenta) and CD68 for macrophages (brown). Small, magenta-stained intracellular bodies co-localizing with CD68+ macrophages are indicated by yellow arrows, confirming intracellular persistence of *C. acnes* within tissue

macrophages. Additionally, IL-1β, a key pro-inflammatory cytokine, is strongly expressed in the affected region. Scale bar = 50μm.

(B) Schematic illustration of the proposed immunopathogenic hypothesis of intracellular *C. acnes* infection in chronic oral inflammatory diseases. Unlike common pathogens that are degraded via phagolysosomal pathway, *C. acnes* may resist degradation, persist within phagosomes, and potentially escape into the cytoplasm. This intracellular persistence may lead to sustained cytokine production and contribute to chronic intractable inflammation.

3.2. Isolation and identification of intracellular infected *C. acnes* in intractable oral inflammatory diseases

Tissue specimens obtained from patient with peri-implantitis and apical periodontitis during surgery were used for bacterial isolation. Each lesion was enzymatically dissociated and enriched for $CD14^+$ cells by magnetic-activated cell sorting (MACS) system (Figure 2A). From the lysates of $CD14^+$ cell population, bacterial colonies were grown under anaerobic conditions and identified as *C. acnes* by PCR amplification of 16S rRNA and *roxP gene*, following by sequencing. The isolate derived from peri-implantitis was designated *C. acnes* D1 strain, and that from apical periodontitis was designated *C. acnes* D2 strain. Clinical information of the patient from whom each strain was isolated is summarized in Table 3, and the corresponding radiographic images and histological images are presented in Figure 1A.

Table 3. Patient information from whom *C. acnes* strain were isolated

Patient Information	*C. acnes* D1 strain	*C. acnes* D2 strain
Age	69 years old	36 years old
Sex	Male	Male
Pre-Medical History	Hepatitis C, Hyperlipidemia	Unremarkable
Affected site	i42, 41, 31	#37 tooth
History of affected lesion	Implant placement and fixed bridge prosthesis (15 years ago)	Root canal treatment and crown prosthesis (about 10 years ago)
Present Illness	- Gingival swelling and peri-implant bone loss - No mobility and tenderness to percussion	- Radiolucent lesion on apex of #37 tooth - 12mm probing depth on mesial side - Vertical root fracture - Mobility (-) and Pain on bite test
Diagnosis	Peri-implantitis	Apical periodontitis with vertical root fracture
Treatment	Removal of Implant fixture	Tooth Extraction

3.3. Intracellular *C. acnes* detection using a customized anti-CA antibody

To directly visualize C. acnes residing within macrophages in intractable oral inflammatory tissues, I generated a customized rabbit poly clonal antibody (anti-CA antibody) using the *C. acnes* D1 strain, which was isolated from peri-implantitis lesion. To validate intracellular detection, apical periodontitis tissue samples were dissociated into single cells, and $CD14^+$ macrophages were enriched by MACS system. Immunofluorescence staining was then performed using CD68 as a macrophage marker, in combination with either the commercial PAB antibody or the newly developed anti-CA antibody. In the $CD14^+$ cell population, small round intracellular bodies were co-stained by both anti-CA and PAB antibodies within $CD68^+$ macrophages (Figure 2C).

These co-localized signals confirmed the intracellular presence of *C. acnes* within a subset of $CD68^+$ macrophages derived from in vivo human apical periodontitis tissues, reinforcing my previous histological observation. In addition, the signal overlap between anti-CA and PAB antibodies validates the specificity and reliability of customized anti-CA antibody. Furthermore, theses findings support the efficacy of CD14-based MACS system in isolating *C. acnes*-harboring macrophages from human in vivo samples.

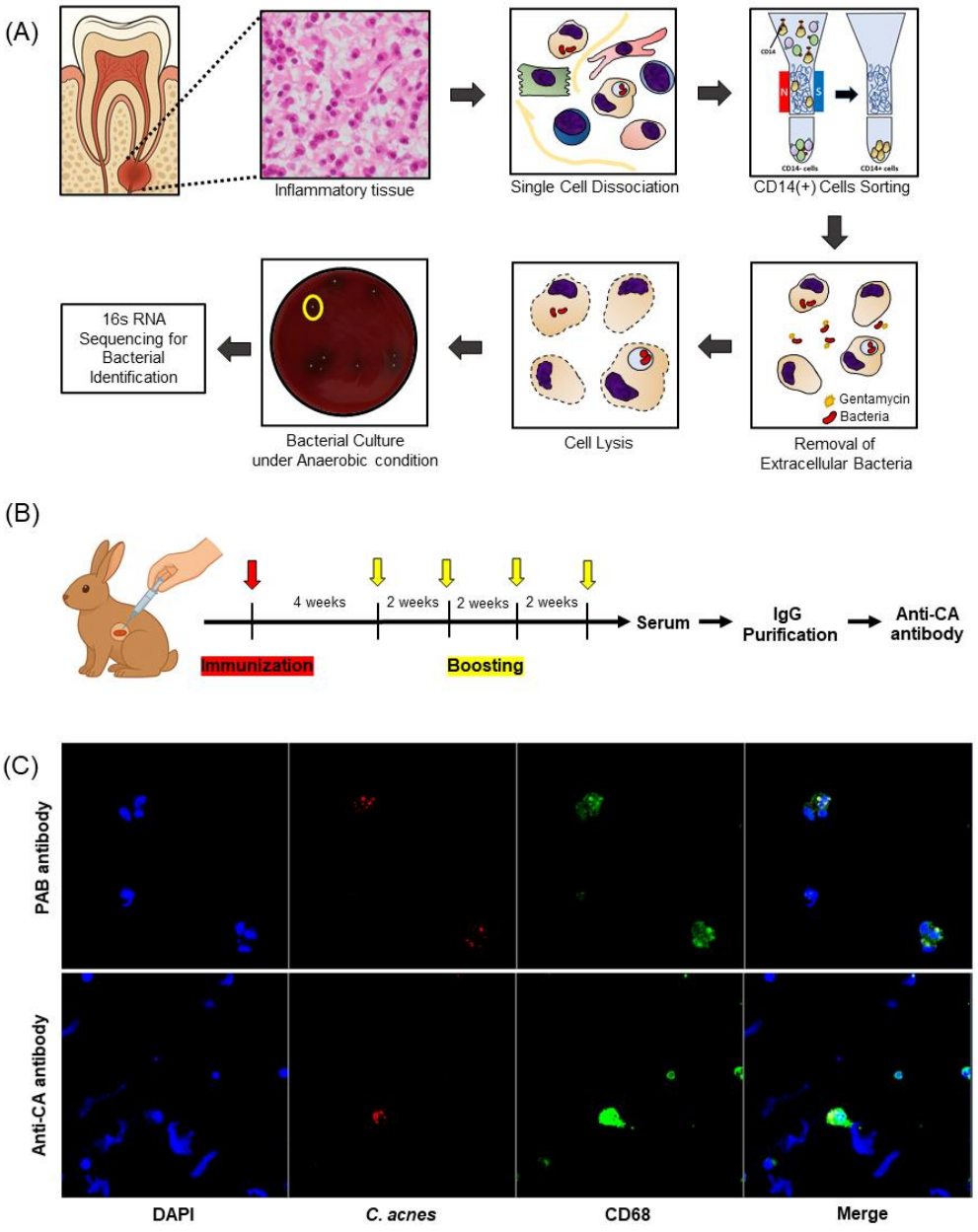

Figure 2. Workflow of intracellular *C. acnes* isolation and detection using a customized polyclonal antibody.

(A) Schematic representation of the experimental workflow for the isolation and identification of intracellular *C. acnes* from human oral inflammatory tissue. Inflammatory tissues were collected during surgical removal and subjected to enzymatic single-cell dissociation. $CD14^+$ cells were isolated using magnetic-activated cell sorting (MACS). To remove extracellular bacteria, cells were cultured in DMEM containing high concentration of antibiotics and subsequently lysed to release intracellular content. Lysates were plated on blood agar under anaerobic conditions for bacterial culture. Colonies were screened by PCR and confirmed as *C. acnes* via 16s rRNA gene sequencing.

(B) Immunization protocol for polyclonal antibody production against *C. acnes*. Rabbits were immunized subcutaneously with live *C. acnes* (CA-D1 strain), followed by four rounds of boosting at two-week intervals. Serum was collected, and IgG was purified to generate the custom anti *C. acnes* (anti-CA) antibody.

(C) Validation of the custom anti-CA antibody in comparison to a commercial PAB antibody. Immunofluorescence staining was performed on $CD14^+$ cells isolated from apical periodontitis lesions. Both PAB and anti-CA antibodies revealed *C. acnes* localization (red) within $CD68^+$ macrophages (green). Nuclei were counterstained with DAPI (blue). Each confocal image represents a field measuring 160 μm x 160 μm..

3.4. Persistent infection of *C. acnes* in macrophage cell lines

Multiple *C. acnes* were observed and localized within membrane-bound vesicles in macrophage-differentiated THP-1 cells on transmission electron microscopy (TEM) at 24 hours post-infection. These vesicles displayed double-membrane-like structures consistent with phagosomes (Figure 3A, left). While some bacteria showed signs of degradation, as indicated by reduced electron density, many *C. acnes* remained structurally intact, suggesting resistance to intracellular digestion. Notably, several *C. acnes* were observed outside of fully enclosed vesicular structures and appeared to be directly exposed to the host cytoplasm (Figure 3A, right). These findings suggest that *C. acnes* not only resists degradation within phagosomes but may also escape into the cytosol, potentially evading host antimicrobial mechanisms and contributing to intracellular persistence.

To investigate how long *C. acnes* can persist inside macrophages, Raw 264.7 cells were infected with the CA-D1 strain (isolated from peri-implantitis) at 100 MOI and sub-cultured for up to 10 days. Immunofluorescence staining revealed that *C. acnes* was detectable in most cells during the early phase (1–2 days post-infection), but the number of infected cells gradually decreased over time. Remarkably, intracellular *C. acnes* was still observed at day 10 post-infection, suggesting prolonged intracellular survival without complete degradation (Figure 3B).

To determine whether the intracellular bacteria observed by IF microscopy remained viable, Raw 264.7 cells infected with *C. acnes* were lysed with 0.05% Triton X-100 at 2 and 4 days post-infection, and lysates were plated on blood agar under anaerobic conditions. Colony formation was observed in the *C. acnes*-infected groups, while no growth was detected in the heat-killed control group, confirming that viable *C. acnes* persisted inside macrophages over time (Figure 3C).

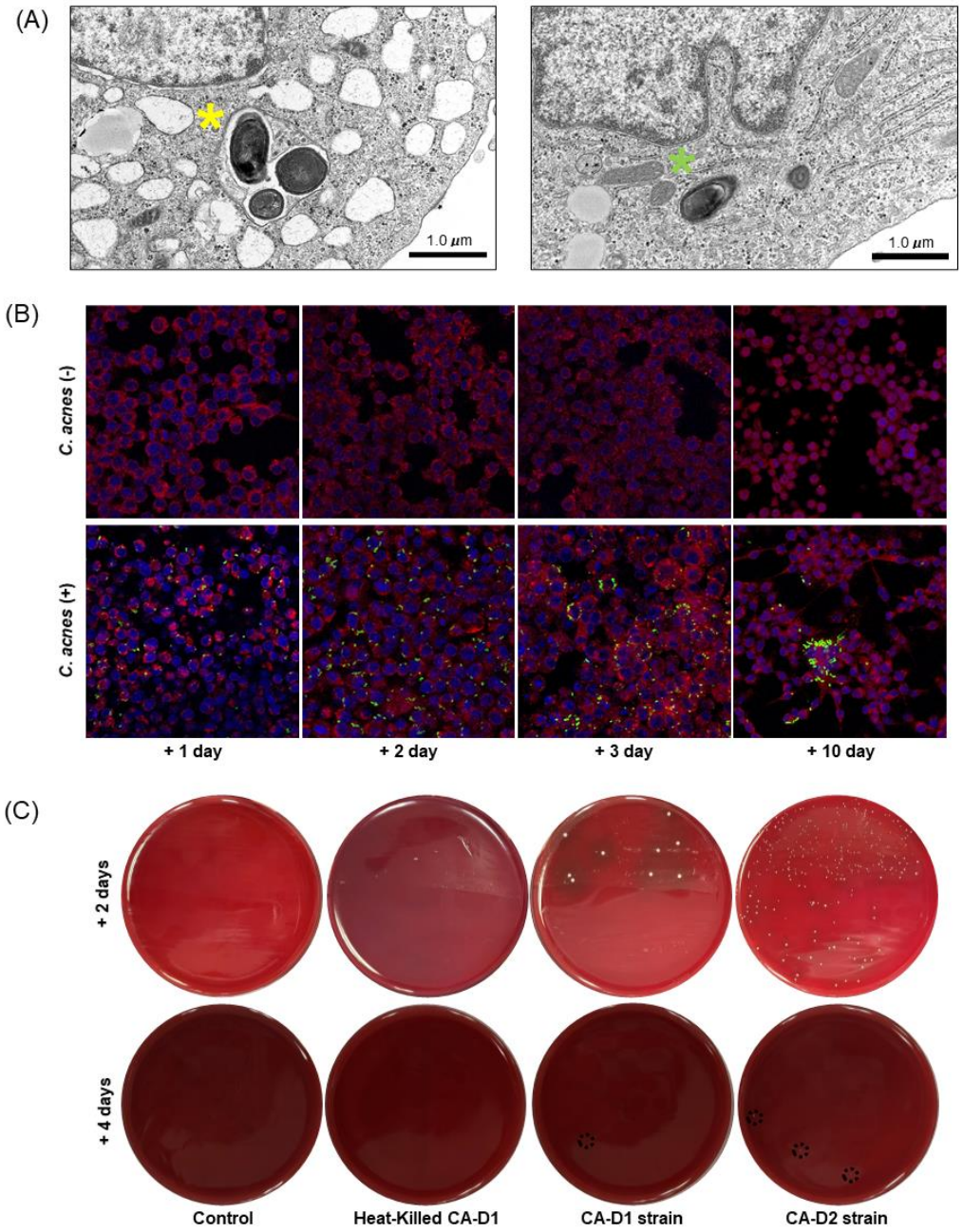

Figure 3. Persistence of intracellular *C. acnes* in macrophage cell lines

(A) Transmission electron microscopy (TEM) of THP-1 cells at 24 hours after *C. acnes* infection. Left: *C. acnes* (yellow asterisk) is enclosed with membrane-bound vesicles resembling phagosome. Right: Some C. acnes (green asterisk) appear to be free in the cytoplasm without being enclosed by a phagosomal membrane, suggesting potential escape from phagolysosomal pathway. Scale bar = 1.0 μm.

(B) Immunofluorescence staining of Raw 264.7 cells infected with *C. acnes* D1 strain across the time points (1, 2, 3, and 10 days post-infection). Cells were stained with PAB antibody (green) to detect *C. acnes*, Rab5 (red), and DAPI (blue) for nuclei. Intracellular *C. acnes* was still detectable at 10 days post infection, indicating long-term persistence in a subset of cells. Uninfected control group (top row) showed no PAB signal. Each confocal image represents a field measuring 160 μm x 160 μm.

(C) Re-colonization of intracellular *C. acnes*. Raw 264.7 cells infected with *C. acnes* D1 or D2 stains were lysed at day 2 and day 4 post-infection and plated on blood agar under anaerobic conditions. Bacterial colonies were observed in live infection groups but not in control or heat-killed groups, confirming the viability and persistence of intracellular *C. acnes.* Colonies observed on day 4 are indicated by black dotted circles.

3.5. Proliferation of intracellular *C. acnes* in macrophages

While examining long-term intracellular persistence of *C. acnes*, we observed that by 10 days post-infection, most Raw 264.7 cells no longer contained visible bacteria; however, a small subset of cells harbored a large number of intracellular *C. acnes* (Figure 4A, upper right). This observation raised the possibility that *C. acnes* may proliferate within certain host cells.

To evaluate this hypothesis, a time-course proliferation assay was performed to monitor intracellular *C. acnes* burden at 24, 48, and 72 hours post-infection using immunofluorescence microscopy. Contrary to expectation the overall PAB signal per cell gradually decreased over time (Figure 4A). Quantitative analysis showed that live *C. acnes* decreased more slowly than heat-killed controls, which dropped markedly after 24 hours. These findings suggest that although intracellular *C. acnes* may persist for extended periods, we did not observe clear evidence of bacterial proliferation within macrophages during the early stages of infection.

3.6. Intercellular transmission of infected *C. acnes* in macrophages

Several intracellular pathogens evade immune clearance and proliferate within host macrophages and subsequently spread to neighboring cells upon host cell lysis. To investigate whether *C. acnes* follows a similar intracellular life cycle, we performed a co-culture assay using infected and un-infected Raw 264.7 cells.

Wild-type Raw 264.7 cells infected with *C. acnes* (D1 or D2 strain) were mixed at a 1:9 ratio with uninfected Raw 264.7-dsRED cells and co-cultured for 5 days. Immunofluorescence analysis revealed that while most *C. acnes* signals (green fluorescence) were detected in dsRED-negative cells, a subset of dsRED-positive cells also harbored intracellular *C. acnes* (Figure 4B). This observation indicates that *C. acnes* is capable of intercellular transmission, likely spreading from infected host cells to neighboring macrophages during the course of infection.

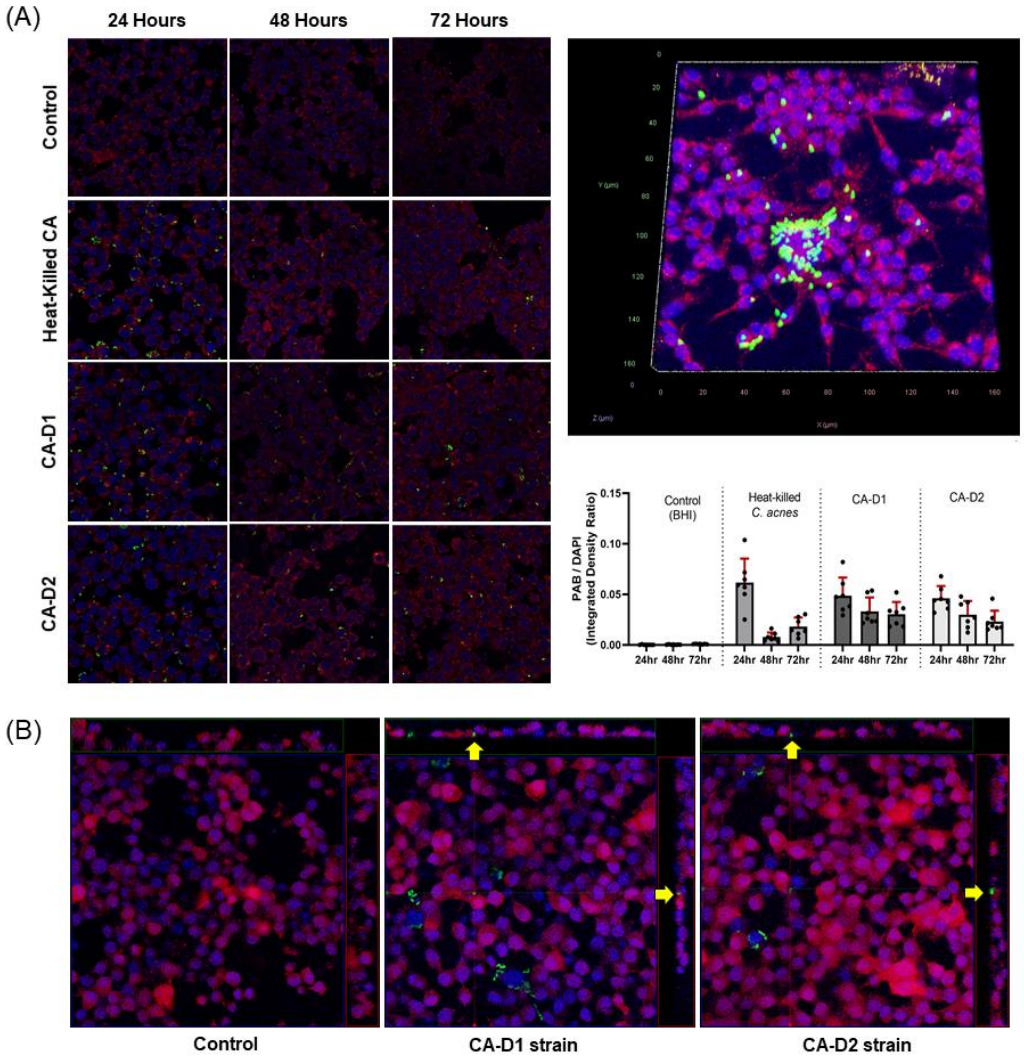

Figure 4. Proliferation and cell-to-cell propagation of intracellular *C. acnes* in macrophages

(A) Immunofluorescence-based quantification of intracellular *C. acnes* proliferation over time. Raw 264.7 cells were infected with live *C. acnes* D1 or D2 strain or heat-killed *C. acnes*, and fixed at 24, 48, and 72 hours post-infection. Cells were stained with PAB antibody (green), Rab5 (red), and DAPI for nuclei (blue). Control and heat-killed groups showed no or minimal signal, while D1 and D2 strain group retained detectable *C. acnes* signal,

with intensity gradually decreasing over time. (Right top) A 3D confocal z-stack projection shows accumulation of intracellular *C. acnes* within a subset of macrophages at 10 days post-infection. (Right bottom: Quantification of intracellular *C. acnes* burden by calculating PAB/DAPI signal ration using ImageJ. Data are presented as mean ± SD (n=5 field per condition). Each confocal image represents a field measuring 160 μm x 160 μm.

(B) Confocal imaging of *C. acnes* spreading between macrophages. Uninfected (control) Raw 264.7 cells were co-cultured with *C. acnes*-infected Raw 264.7 cells for 5 days. Z-stack projection (XZ and YZ planes) demonstrate PAB-positive *C. acnes* (green) localized within both infected and neighboring, previously uninfected cells (indicated by yellow arrow), suggesting intercellular propagation. Each confocal image represents a field measuring 160 μm x 160 μm.

3.7. Proliferation and viability of *C. acnes*-infected Raw 264.7 cells

To investigate how *C. acnes* infection affects host macrophage physiology, we performed both proliferation and viability assay. Morphologically, infected Raw 264.7 cells displays a distinct change compared to control cells: while uninfected cells maintain a round, monocyte-like shape, infected cells exhibit more cellular projections, activated appearance (Figure 5A).

Cell proliferation, assessed by trypan blue exclusion assay, revealed that *C. acnes*-infected cells showed a slower growth rate over time compared to uninfected control (Figure 5A). However, when assessing cytotoxicity using MTT assay, no significant reduction in viability was observed across MOI conditions when compared to the control (Figure 5B). Interestingly, cells infected at lower MOIs exhibited a statistically significant increase in viability. These results indicate that *C. acnes* infection does not induce overt cytotoxicity in Raw 264.7 macrophages but may promote M1-polarization-like morphological changes and decelerate cellular proliferation.

3.8. Pro-inflammatory response of *C. acnes*-infected Raw 264.7 cells

Raw 264.7 cells infected with *C. acnes* D1 and D2 strains exhibited strong pro-inflammatory responses. RT-qPCR analysis revealed significantly upregulated mRNA expression of key inflammatory cytokines and chemokines, including IL-1α, IL-1β, IL-6, IL-23, TNF- α, CCL2, and CSF2 (Figure 5C). Cytokine Array analysis revealed the significantly increased level of cytokines and chemokines, including GCSF, IL-6, CCL2, CCL5, and TNF-RII in the *C. acnes*-infected Raw 264.7 cells (Figure 5D). Upregulation of these cytokines induced by D1 and D2 strain was not remarkably differed.

Bulk RNA sequencing further confirmed this inflammatory activation. In total, 1,672 genes were upregulated and 1,464 gene were downregulated in *C. acnes*-infected cells compared to the uninfected control (Figure 6A). However, when comparing intracellular *C. acnes* strain (C1, D1, D2) to extracellular strains (KBN12P07016, KBN12P05481, KBN12P07215), only minimal gene expression differences were identified (4 upregulated and 2 downregulated gene), suggesting that there were no significant transcriptional differences between two groups (Figure 6B). This implies that the inflammatory response is largely attributable to *C. acnes* exposure itself rather than the

anatomical origin of the isolated strains.

KEGG pathway enrichment analysis of the differentially expressed genes revealed substantial activation of immune-related pathways among upregulated genes, including cytokine-cytokine receptor interaction, inflammatory signaling and microbial infection responses (Figure 6C, left panel). Notably, the cytosolic DNA-sensing pathway and the tuberculosis-related pathway were also enriched, suggesting possible activation of host defense mechanisms targeting intracellular pathogens. In contrast, downregulated genes were predominantly associated with cell cycle-related pathways (Figure 6C, right panel), which is consistent with the reduced cell proliferation observed in *C. acnes*-infected Raw 264.7 cells (Figure 5A).

To elucidate the upstream transcriptional regulators of *C. acnes*-induced inflammation, we estimated transcription factor (TF) activities from bulk RNA sequencing data using the CollecTRI regulatory network. The TF activity scores revealed significant upregulation of inflammation-associated TFs, including Nfkb1, Spi1, Stat1, and Jun, while TFs related to cell cycle progression and proliferation, such as E2f4, E2f1, Myc, and E2f3, were notably downregulated (Figure 6D). Network analysis of the top activated and suppressed TFs confirmed that inflammation-related TFs exhibited dense interaction with target genes (Figure 6E). Further inspection of individual target gene volcano plots revealed that TFs like Nfkb1, Spi1, Stat1, and Jun shared commonly activated downstream targets, including Il1rn, PtgS2, Mmp9, Ccl2, and Upp1 (Figure 6F).

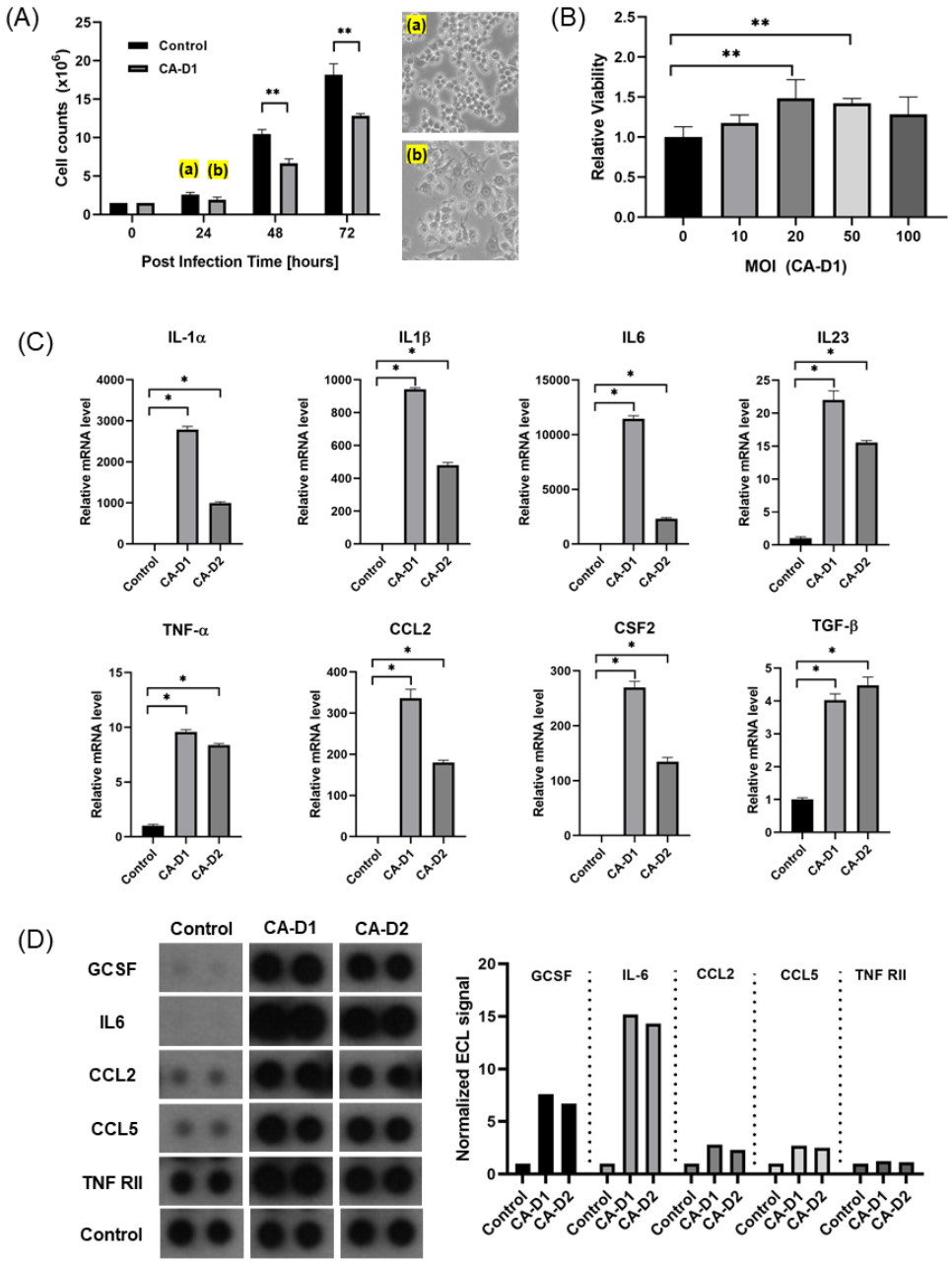

Figure5. Host macrophage response to intracellular *C. acnes* infection

(A) Proliferation assay of Raw 264.7 cells infected with *C. acnes* D1 strains. Cell counts were measured at 0 ,24, 48, and 72 hours post-infection using trypan blue assay. Infected cell showed significantly reduced proliferation compared to control. Phase contrast images on the right show morphological changes: (a) control group exhibiting round monocyte-like morphology; (b) *C. acnes* infected cells showing irregular shape and pseudopod extension.

(B) Cell viability test after 24 hours of infection with increasing MOIs (0, 10, 20, 50, 100) of *C. acnes* D1 strain. Viability was assessed using MTT assay. No significant cytotoxicity was observed, and mild increases in viability were noted at lower MOIs.

(C) Relative mRNA expression of pro-inflammatory cytokines and chemokines measured by RT-qPCR 24 hours post-infection with *C. acnes* D1 and D2 strains.

(D) Cytokine array revealed significantly elevated protein level of GCSF, IL6, CCL2, CCL5 and TNF RII. The difference between D1 and D2 strain on cytokine production was not observed.

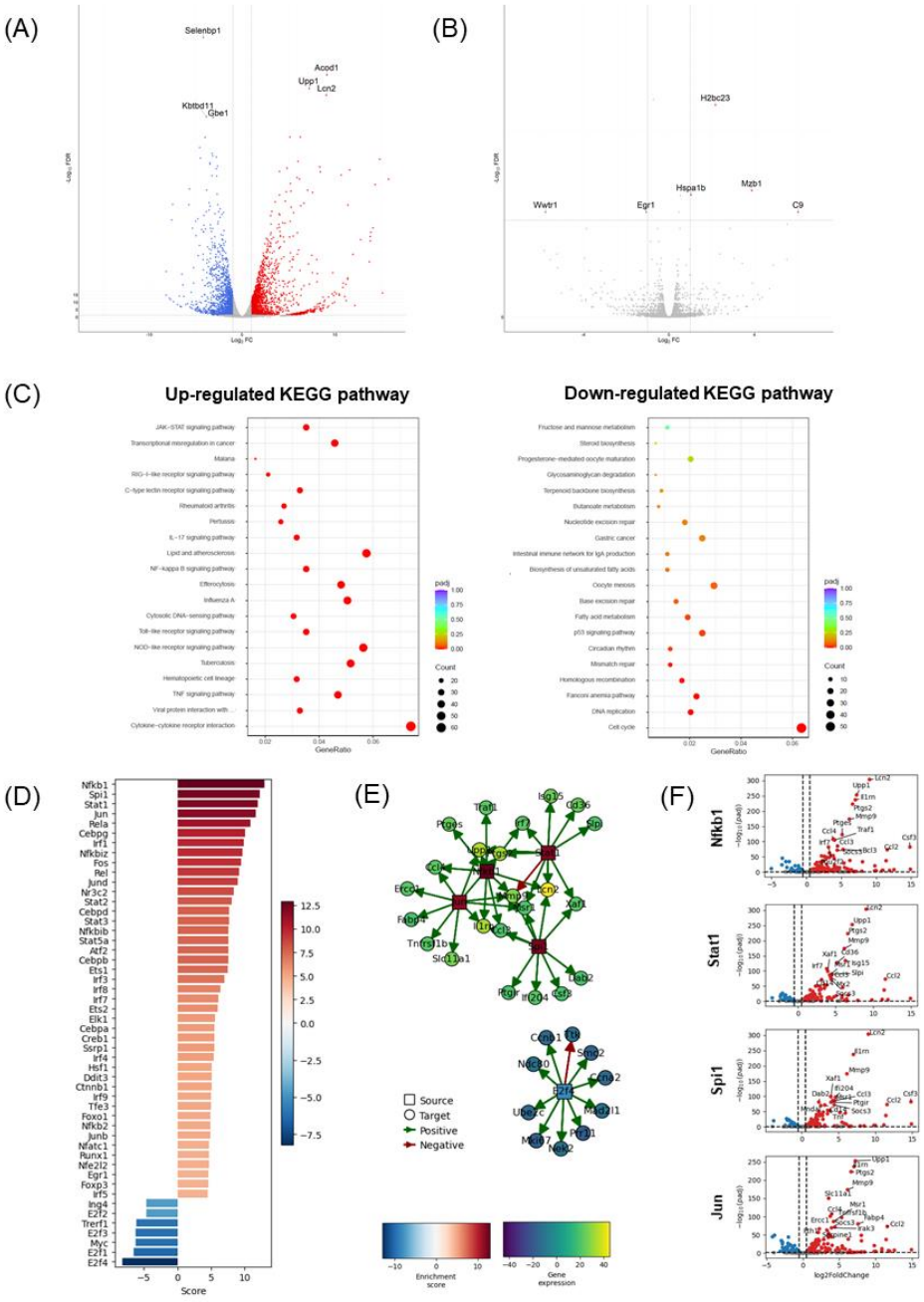

Figure 6. Transcriptomic profiling of *C. acnes*-infected Raw 264.7 macrophages by bulk RNA sequencing

(A) Volcano plot showing differentially expressed genes (DEGs) between all *C. acnes*-infected group and uninfected control group. A total of 1,672 gene were significantly upregulated and 1,464 genes were downregulated.

(B) Volcano plot comparing gene expression between intracellular C. acnes strains (C1, D1, D2) and extracellular strain (KBN12P07016, KBN12P05481, KBN12P07215). Only a few DEGs were detected (4 upregulated, 2 downregulated), suggesting minimal transcriptional difference based on strain origin.

(C) KEGG pathway enrichment analysis of DEGs from panel (A). Significantly upregulated pathways (left panel) include immune and inflammatory response such as cytokine-cytokine receptor interaction, various inflammatory signaling, and microbial infection-related pathways. Notably, the tuberculosis-related pathway was also enriched, implying activation of host defense mechanisms against intracellular pathogen. Downregulated pathways are predominantly associated with cell proliferation, including cell cycle, DNA replication, and various DNA repair mechanisms, consistent with the observed decreased in cell proliferation upon C. acnes infection

The x-axis indicates the gene ratio (the number of differentially expressed genes involved in a given pathway divided by the total number of gene in that pathway). The size of each dot represents the number of genes enriched in corresponding pathway (gene count), and the color gradient indicates the statistical significance (adjusted p-value), with red indicating greater significance.

(D) Inferred activity scores of transcription factors using CollecTRI regulatory networks. Red bars indicated upregulated TFs; blue bars indicate downregulated TFs.

(E) Network diagram of representative TFs with the highest (red) and lowest (blue) activity scores; node colors of target gene reflect gene expression levels.

(F) Volcano plots showing log2 fold change versus adjusted p-value (padj) of target genes regulated by Nfkb1, Spi1, Stat1, and Jun. Genes significantly upregulated and associated with inflammatory responses (e.g., Il1rn, PtgS2, Mmp9, Ccl2) are labeled.

3.9. Sarcoidosis-like granulomatous inflammation induced by subcutaneous injection of *C. acnes* in mice model

To investigate the in vivo inflammatory potential of *C. acnes* strains isolated from intractable oral inflammatory diseases, we subcutaneously injected mice with live or heat-killed *C. acnes* D1 and D2 strain (Figure 7A). Histopathological analysis of the injected sites revealed granulomatous inflammation in all *C. acnes* experimental groups, including those injected with heat-killed bacteria (Figure 7B). While both live and heat-killed *C. acnes* strain induced granulomatous inflammation, central necrosis was observed much frequently in lesions injected with live *C. acnes,* implying more aggressive and active immune response (Figure 7B). Granuloma formation is typically triggered by persistent pathogens or indigestible antigens, suggesting *C. acnes* may elicit a chronic immune response similar to those of other intracellular pathogens.

Immunohistochemical staining for *C. acnes* (anti-CA antibody) and CD68 revealed that bacteria persisted intracellularly within macrophages at the inflammation sites even 7 days after the final injection (Figure 7C, panels ① and ②), supporting the notion of long-term survival of *C. acnes* in vivo. Moreover, IHC staining for pro-inflammatory cytokines-including IL-1β, IL-23, and TNF-α-demonstrated marked upregulation of these cytokines in the affected tissues, further indicating a sustained inflammatory response (Figure 8A and 8B). These results demonstrate that intracellular persistence of *C. acnes* correlates with sustained granulomatous inflammation and heightened cytokine expression, resembling the host response to other chronic intracellular pathogens.

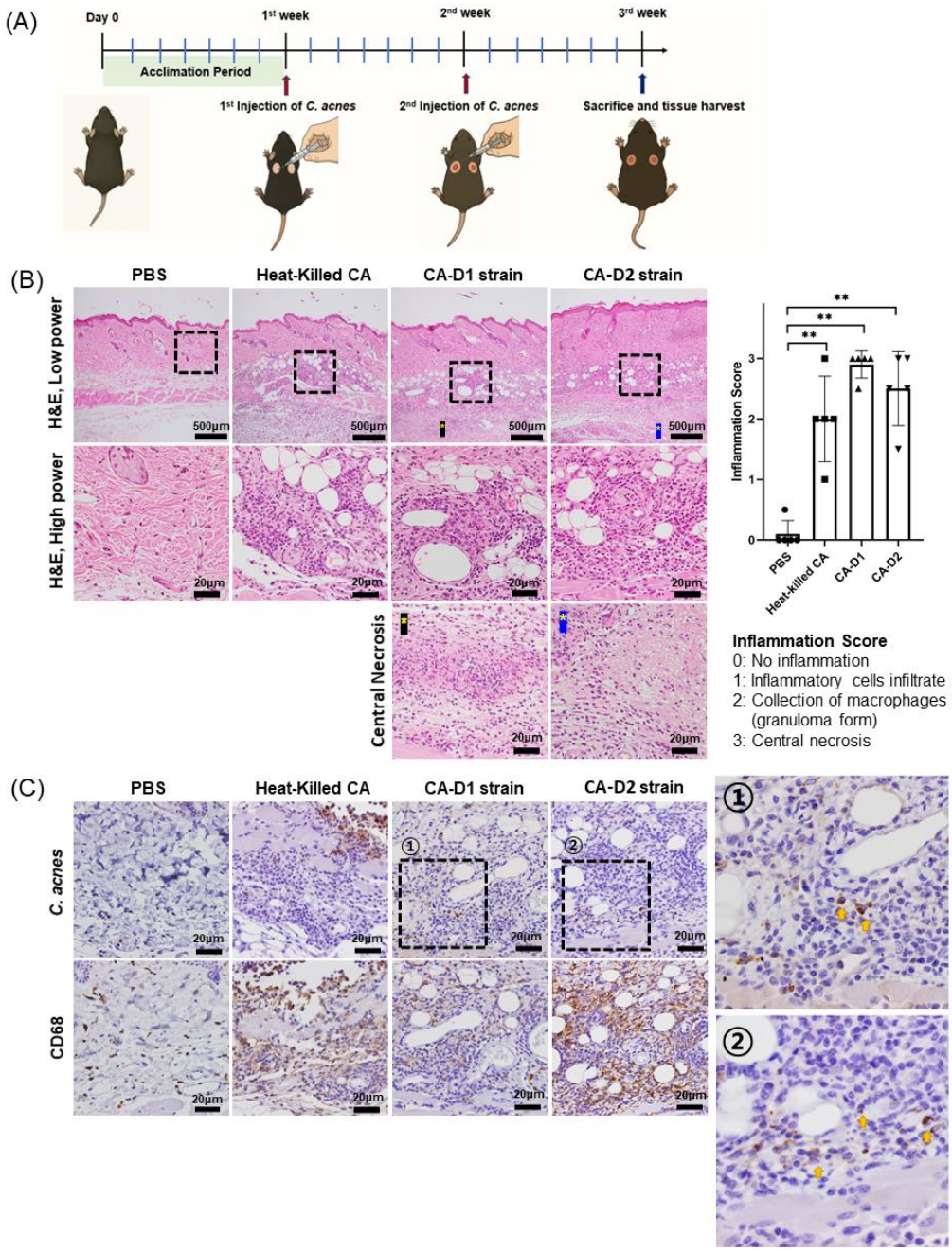

Figure 7. Subcutaneous injection of *C. acnes* induces granulomatous inflammation in murine

model

(A) Schematic timeline of the murine subcutaneous injection protocol

(B) Representative histological and immunohistochemical images of skin tissues from each group. The black dotted box in the low-magnification image corresponds to the region shown in the high-magnification panel. H&E image revealed no inflammation in PBS group, and more prominent inflammatory cell infiltrates and granuloma in the heat-killed *C. acnes* group. Both *C. acnes* D1 and D2 strain-injected groups showed granulomatous inflammation and central necrosis (yellow asterisk). The scale bar for the low-magnification images is 500μm, and for the high-magnification images is 20μm.

Inflammation scoring was performed on H&E-stained section using a semiquantitative scale (0-3). Statistical analysis was performed by comparing each group to the control (PBS group); statistical significance: $p < 0.01$ (**).

(C) Immunohistochemical staining using anti-CA antibody and anti-CD68 antibody confirmed the presence of *C. acnes* within $CD68^+$ macrophages in infected group. The scale bar is 500μm.

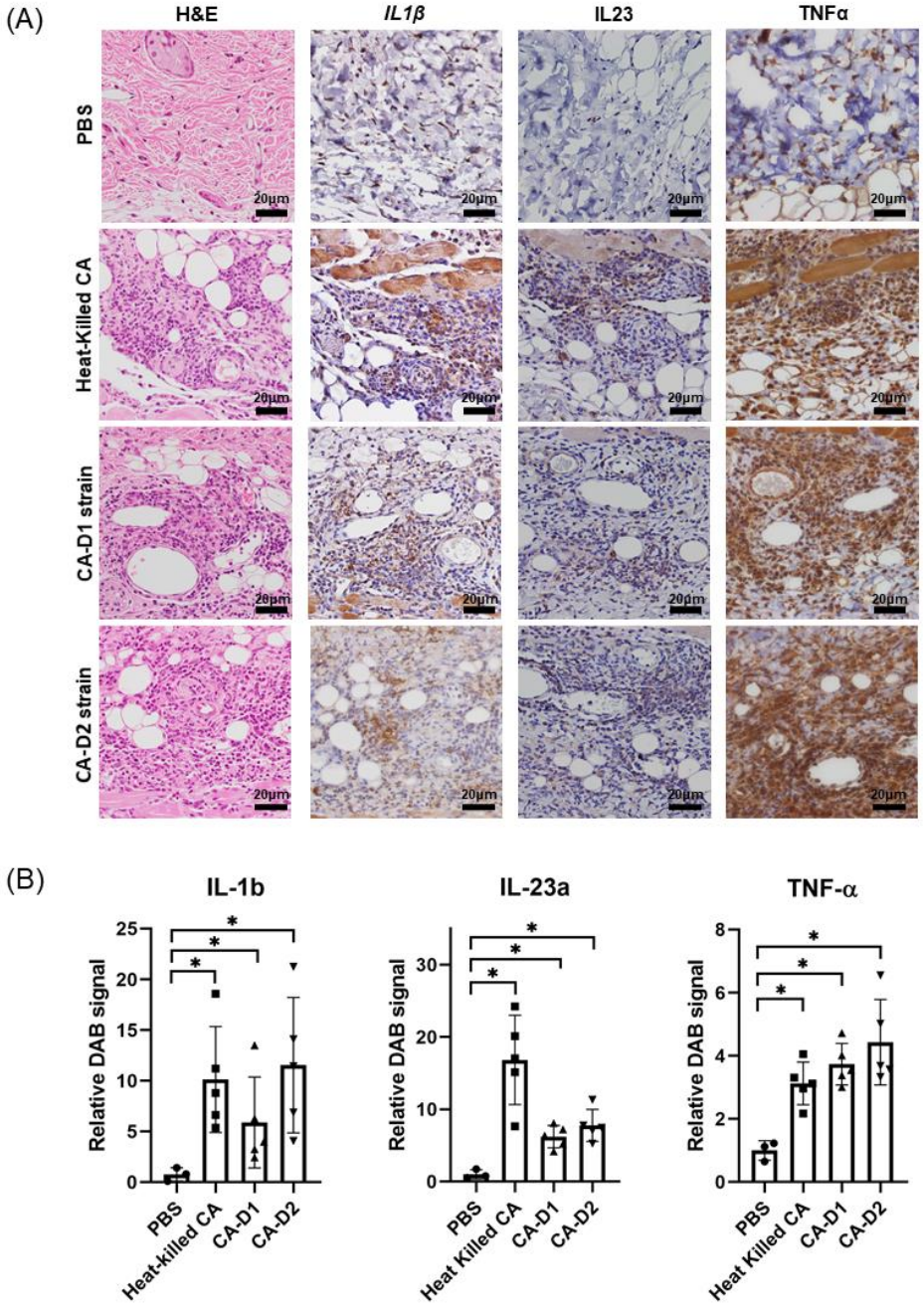

Figure 8. Inflammatory cytokine expression in *C. acnes*-injected mouse skin tissues.

(A) Immunohistochemical staining for pro-inflammatory cytokines (IL-1β, IL-23α, and TNF-α) revealed enhanced expression in tissues injected with heat-killed or live *C. acnes*, particularly in the D1 and D2 groups. Scale bar = 20 μm

(B) Quantitative analysis of DAB signal intensity from immunohistochemistry for IL-1β, IL-23a, and TNF-α. Signal intensity was measured from five randomly selected regions per tissue section using ImageJ software. Both *C. acnes* D1 and D2 strains showed higher cytokine expression compared to PBS. Statistical analysis was performed by comparing each group to the control (PBS group); statistical significance: $p < 0.05$ (*).

4. Discussion

Although *Cutibacterium acnes (C. acnes)* is a common commensal bacterium of the skin and oral mucosa, it can cause infection in some inflammatory conditions. Whether this pathogenic behavior is determined by bacterial virulence factors, host susceptibility, or a combination of both remains unresolved. *C. acnes* exhibits considerable genetic diverse, with multiple phylogenetic subsets. Previous studies have suggested that strains responsible for acne vulgaris differ from those associated with deep tissue infection such as prosthetic joint infections and other post-surgery infections, but it is still controversial (Mayslich et al., 2021). Type IA *C. acnes* predominate in skin microbiota and acne vulgaris, whereas type IB and II *C. acnes* are more commonly in prosthetic joints infection (PJI) (McDowell et al., 2012) . In rat model study, type II and III *C. acnes* can persist on the surface of orthopedic device, inducing inflammation and osteolysis (Stadelmann et al., 2020). In endodontic lesions, Niazi et al. classified *C. acnes* isolated by partial sequencing of recA gene, and type I was predominant (44 out of 47) and type II was less (3 out of 47) (Niazi et al., 2016).

The *C. acnes* strains isolated in this study were classified by Single-Locus Sequence-Typing (SLST), revealing that the D1 strain belonged to type II and the D2 strain to type III (data are not shown), which are distinct from the commonly skin-associated type I strains (Scholz et al., 2014). However, due to the limited number of strains analyzed, it is insufficient to draw definitive conclusions regarding the relationship between intracellular *C. acnes* subtypes and their pathogenic roles in intractable oral inflammatory lesions.

The ability of a microorganism to survive within host cells is a critical determinant of its pathogenic potential. Following Eishi's seminal observation of *C. acnes* residing within granulomas and surrounding macrophages in sarcoidosis-affected lymph nodes and lungs (Negi et al., 2012), several studies have attempted to explore this intracellular behavior. However, unlike well-characterized intracellular pathogens such as *Mycobacterium tuberculosis*, the detailed mechanisms by which *C. acnes* persists intracellularly remain poorly understood. Some investigations have addressed whether specific subtypes of *C. acnes* are associated with intracellular invasiveness. Eishi's group reported that although there was no clear difference in invasiveness between *C. acnes* strains isolated from sarcoidosis and non-sarcoidosis cases, serotype I strains demonstrated higher intracellular infectivity (71%) compared to serotype II strains (0%), possibly due to mutations in the

PAmce or PAp60 genes (Furukawa et al., 2009). Furthermore, genome analysis of the C1 strain isolated from a cutaneous sarcoidosis lesion revealed a novel insertion sequence found in the majority of MLST ST26 isolates (12 out of 13), which may be linked to their cell invasiveness and granuloma-inducing capacity (Minegishi et al., 2015)

In the present study, we infected macrophages with six different *C. acnes* strains (although data for non-D1/D2 strains are not shown). All strains demonstrated the ability to persist intracellularly, regardless of their subtype. Additionally, bulk RNA sequencing revealed no significant differences in the host transcriptomic response between intracellular and extracellular strains. These findings suggest that the pathogenicity of *C. acnes* cannot be fully explained by phylogenetic subtype alone, and further studies are needed to resolve the complex relationship between strain diversity and intracellular behavior.

One hallmark of intracellular pathogens is their ability to replicate within host cells. However, in our study, we did not quantify intracellular proliferation of *C. acnes*. It is plausible that intracellular replication may occur under specific conditions favorable to bacterial survival and growth. In vivo, macrophage numbers typically increase not by cell division but through monocyte recruitment and differentiation. However, Raw 264.7 cells used in this study have a high proliferation rate in vitro. If *C. acnes* does not replicate efficiently within individual macrophages during early infection stages, then the overall bacterial burden per cell may appear to decrease when averaged across the expanding population. Nonetheless, the observation that numerous *C. acnes* are present within a single large cell, even after considerable time has passed since infection, suggests that the bacteria are still multiplying in a small number of cells. Further studies should carefully design infection models that control for host cell proliferation and use alternative methods, such as single-cell bacterial load quantification, to verify intracellular replication.

The mechanisms by which *C. acnes* survives intracellularly remain poorly understood. Our data suggest that *C. acnes* can remain intact within phagosomal compartments, and in some cases, localize freely in the cytosol in electron microscopy. Fischer et al. argued that *C. acnes* could escape into the cytosol or neutralize the pH within the phagosome, as phagosomes were acidified and disappeared 6 hours after infection in THP-1 cells infected with *C. acnes* (Fischer et al., 2013). He also argued that fusion with lysosomes would not occur, as co-localization with LAMP1 or cathepsin D was not observed (Fischer et al., 2013). On the other hand, Nakamura et al. claimed that after

infection with *C. acnes* in Raw 264.7 cells, LAMP-1 positive vacuoles were present, and no viable *C. acnes* were found at 3 days (Nakamura et al., 2016). However, *C. acnes* was observed to be freely present in the cytoplasm, and it was thought that it escaped the phagosome, as autophage was induced (Nakamura et al., 2016). Another Fischer argues that the type I interferon response induced by *C. acnes* infection is induced via the cGAS-Sting pathway, which senses intracytoplasmic DNA (Fischer et al., 2020). The intracellular infection of *C. acnes* shows different results depending on the cell line, MOI, *C. acnes* strain used, etc., but in common, escape of *C. acnes* into the cytoplasm is considered to be a potential mechanism of intracellular infection.

An intriguing finding of this study was that heat-killed *C. acnes* induced granulomatous inflammation in vivo model, similar to live bacteria. The capacity of trigger granulomatous inflammation has remained controversial. In a previous murine study, pulmonary granulomas were effectively induced by live *C. acnes*, but not by heat-killed counterparts. Moreover, granuloma formation was enriched in mice deficient in *MyD88* and *Cybb*, suggesting a possible association between impaired bacterial clearance and granuloma development (Werner et al., 2017). In contrast, other studies have demonstrated that sensitization with recombinant trigger factor protein (RP35) derived from *C. acnes* was sufficient to induce sarcoidosis-like pulmonary granuloma in mice (Iio et al., 2010; Minami et al., 2003). Furthermore, pulmonary granulomas developed following the adoptive transfer of CD4+ T cells from draining lymph nodes of mice sensitized with heat-killed *C. acnes* (Nishiwaki et al., 2004). These findings imply that granulomatous inflammation can be elicited by hypersensitivity reaction s to specific *C. acnes*-derived antigen, potentially contributing to sarcoidosis pathogenesis.

The significance of our study lies in highlighting the role of intracellular *C. acnes* in chronic refractory inflammation. Conventional approaches to infection management, including systemic antibiotics or surgical debridement, may be insufficient when intracellular pathogens are involved. In the oral cavity, where bacterial colonization is dense and diverse, targeting intracellular bacteria poses a unique challenge. While antibiotics can resolve acute inflammation, latent intracellular bacteria such as *C. acnes* may persist and reactivate, contributing to recurrence and disease progression. Intracellular *C. acnes* is likely to exhibit resistance to both antibiotics and host immune mechanisms. Thus, identifying antibiotics capable of penetrating host cells and targeting intracellular *C. acnes* is essential.

This study provides a basis for reevaluating the role of *C. acnes* as an intracellular pathogen and a potential driver of chronic granulomatous inflammation. Further research should aim to uncover the molecular mechanisms of intracellular survival and screen for antibiotics with intracellular efficacy. Given the frequency of idiopathic granulomatous inflammation in various tissues, including the oral cavity, incorporating *C. acnes* diagnostics in routine pathological evaluation may improve treatment outcomes. Ultimately, we propose that targeting intracellular *C. acnes* could form the basis of a novel therapeutic strategy for refractory oral inflammatory diseases.

5. Conclusion

The study demonstrates the *Cutibacterium acnes* isolated from intractable oral inflammatory diseases can persist within macrophages without undergoing complete degradation, induce strong pro-inflammatory responses, and disseminate to neighboring cells, indicating its capacity for intracellular survival and intercellular transmission. In vivo, intracellular *C. acnes* infection triggered granulomatous inflammation and sustained cytokine expression, further supporting its role as a persistent intracellular pathogen. Its long-term intracellular viability and capacity for intercellular spread suggest mechanisms of immune evasion that may contribute to chronic and refractory inflammation. These findings highlight the importance of targeting intracellular *C. acnes* in the diagnosis and treatment of intractable oral inflammatory diseases and warrant further investigation into host-pathogen interactions and effective intracellular-targeted therapies.

References

Ashida, S., Kawada, C., Tanaka, H., Kurabayashi, A., Yagyu, K.-i., Sakamoto, S., Maejima, K., Miyano, S., Daibata, M., Nakagawa, H., & Inoue, K. (2024). Cutibacterium acnes invades prostate epithelial cells to induce BRCAness as a possible pathogen of prostate cancer. *The Prostate*, *84*(11), 1056-1066. https://doi.org/https://doi.org/10.1002/pros.24723

Bae, Y., Ito, T., Iida, T., Uchida, K., Sekine, M., Nakajima, Y., Kumagai, J., Yokoyama, T., Kawachi, H., Akashi, T., & Eishi, Y. (2014). Intracellular Propionibacterium acnes infection in glandular epithelium and stromal macrophages of the prostate with or without cancer. *PLoS One*, *9*(2), e90324. https://doi.org/10.1371/journal.pone.0090324

Capoor, M. N., Konieczna, A., McDowell, A., Ruzicka, F., Smrcka, M., Jancalek, R., Maca, K., Lujc, M., Ahmed, F. S., Birkenmaier, C., Dudli, S., & Slaby, O. (2021). Pro-Inflammatory and Neurotrophic Factor Responses of Cells Derived from Degenerative Human Intervertebral Discs to the Opportunistic Pathogen Cutibacterium acnes. *Int J Mol Sci*, *22*(5). https://doi.org/10.3390/ijms22052347

Davidsson, S., Carlsson, J., Greenberg, L., Wijkander, J., Söderquist, B., & Erlandsson, A. (2021). Cutibacterium acnes Induces the Expression of Immunosuppressive Genes in Macrophages and is Associated with an Increase of Regulatory T-Cells in Prostate Cancer. *Microbiology Spectrum*, *9*(3), e01497-01421. https://doi.org/10.1128/spectrum.01497-21

Deo, P. N., & Deshmukh, R. (2019). Oral microbiome: Unveiling the fundamentals. *J Oral Maxillofac Pathol*, *23*(1), 122-128. https://doi.org/10.4103/jomfp.JOMFP_304_18

Eishi, Y. (2013). Etiologic link between sarcoidosis and Propionibacterium acnes. *Respiratory Investigation*, *51*(2), 56-68. https://doi.org/https://doi.org/10.1016/j.resinv.2013.01.001

Eishi, Y. (2023). Potential Association of Cutibacterium acnes with Sarcoidosis as an Endogenous Hypersensitivity Infection. *Microorganisms*, *11*(2). https://doi.org/10.3390/microorganisms11020289

Fischer, K., Tschismarov, R., Pilz, A., Straubinger, S., Carotta, S., McDowell, A., & Decker, T. (2020). Cutibacterium acnes Infection Induces Type I Interferon Synthesis Through the cGAS-STING Pathway. *Front Immunol*, *11*, 571334. https://doi.org/10.3389/fimmu.2020.571334

Fischer, N., Mak, T. N., Shinohara, D. B., Sfanos, K. S., Meyer, T. F., & Brüggemann, H. (2013). Deciphering the Intracellular Fate of Propionibacterium acnes in Macrophages. *BioMed Research International*, *2013*(1), 603046.

https://doi.org/https://doi.org/10.1155/2013/603046

Furukawa, A., Uchida, K., Ishige, Y., Ishige, I., Kobayashi, I., Takemura, T., Yokoyama, T., Iwai, K., Watanabe, K., Shimizu, S., Ishida, N., Suzuki, Y., Suzuki, T., Yamada, T., Ito, T., & Eishi, Y. (2009). Characterization of Propionibacterium acnes isolates from sarcoid and non-sarcoid tissues with special reference to cell invasiveness, serotype, and trigger factor gene polymorphism. *Microbial Pathogenesis*, *46*(2), 80-87. https://doi.org/https://doi.org/10.1016/j.micpath.2008.10.013

Han, D., Song, S. H., Han, S. Y., Cho, N. Y., Yook, J. I., Lee, J. S., & Cho, E. S. (2024). Cutibacterium acnes-induced Facial Granulomas Associated with the Clinical Course of Distinct Dental Infections: A Case Report. *The Korean Journal of Oral and Maxillofacial Pathology*, *48*(6), 105-113.

Iio, K., Iio, T. U., Okui, Y., Ichikawa, H., Tanimoto, Y., Miyahara, N., Kanehiro, A., Tanimoto, M., Nakata, Y., & Kataoka, M. (2010). Experimental pulmonary granuloma mimicking sarcoidosis induced by Propionibacterium acnes in mice. *Acta Med Okayama*, *64*(2), 75-83. https://doi.org/10.18926/amo/32852

Mayslich, C., Grange, P. A., & Dupin, N. (2021). Cutibacterium acnes as an Opportunistic Pathogen: An Update of Its Virulence-Associated Factors. *Microorganisms*, *9*(2). https://doi.org/10.3390/microorganisms9020303

McDowell, A., Barnard, E., Nagy, I., Gao, A., Tomida, S., Li, H., Eady, A., Cove, J., Nord, C. E., & Patrick, S. (2012). An expanded multilocus sequence typing scheme for propionibacterium acnes: investigation of 'pathogenic', 'commensal' and antibiotic resistant strains. *PLoS One*, *7*(7), e41480. https://doi.org/10.1371/journal.pone.0041480

Minami, J., Eishi, Y., Ishige, Y., Kobayashi, I., Ishige, I., Kobayashi, D., Ando, N., Uchida, K., Ikeda, S., Sorimachi, N., Karasuyama, H., Takemura, T., Takizawa, T., & Koike, M. (2003). Pulmonary granulomas caused experimentally in mice by a recombinant trigger-factor protein of Propionibacterium acnes. *J Med Dent Sci*, *50*(4), 265-274.

Minegishi, K., Watanabe, T., Furukawa, A., Uchida, K., Suzuki, Y., Akashi, T., Maruyama, F., Nakagawa, I., & Eishi, Y. (2015). Genetic profiles of Propionibacterium acnes and identification of a unique transposon with novel insertion sequences in sarcoid and non-sarcoid isolates. *Scientific Reports*, *5*(1), 9832. https://doi.org/10.1038/srep09832

Nakamura, T., Furukawa, A., Uchida, K., Ogawa, T., Tamura, T., Sakonishi, D., Wada, Y., Suzuki, Y., Ishige, Y., Minami, J., Akashi, T., & Eishi, Y. (2016). Autophagy Induced by Intracellular Infection of Propionibacterium acnes. *PLoS One*, *11*(5), e0156298. https://doi.org/10.1371/journal.pone.0156298

Negi, M., Takemura, T., Guzman, J., Uchida, K., Furukawa, A., Suzuki, Y., Iida, T., Ishige, I.,

Minami, J., Yamada, T., Kawachi, H., Costabel, U., & Eishi, Y. (2012). Localization of Propionibacterium acnes in granulomas supports a possible etiologic link between sarcoidosis and the bacterium. *Modern Pathology*, *25*(9), 1284-1297. https://doi.org/10.1038/modpathol.2012.80

Niazi, S. A., Al Kharusi, H. S., Patel, S., Bruce, K., Beighton, D., Foschi, F., & Mannocci, F. (2016). Isolation of Propionibacterium acnes among the microbiota of primary endodontic infections with and without intraoral communication. *Clin Oral Investig*, *20*(8), 2149-2160. https://doi.org/10.1007/s00784-016-1739-x

Nishiwaki, T., Yoneyama, H., Eishi, Y., Matsuo, N., Tatsumi, K., Kimura, H., Kuriyama, T., & Matsushima, K. (2004). Indigenous pulmonary Propionibacterium acnes primes the host in the development of sarcoid-like pulmonary granulomatosis in mice. *Am J Pathol*, *165*(2), 631-639. https://doi.org/10.1016/s0002-9440(10)63327-5

Park, J. Y., Han, D., Park, Y., Cho, E. S., In Yook, J., & Lee, J. S. (2024). Intracellular infection of Cutibacterium acnes in macrophages of extensive peri-implantitis lesions: A clinical case series. *Clin Implant Dent Relat Res*, *26*(6), 1126-1134. https://doi.org/10.1111/cid.13367

Persson, G. R., & Renvert, S. (2014). Cluster of bacteria associated with peri-implantitis. *Clin Implant Dent Relat Res*, *16*(6), 783-793. https://doi.org/10.1111/cid.12052

Scholz, C. F. P., Jensen, A., Lomholt, H. B., Brüggemann, H., & Kilian, M. (2014). A Novel High-Resolution Single Locus Sequence Typing Scheme for Mixed Populations of Propionibacterium acnes In Vivo. *PLoS One*, *9*(8), e104199. https://doi.org/10.1371/journal.pone.0104199

Stadelmann, V. A., Thompson, K., Zeiter, S., Camenisch, K., Styger, U., Patrick, S., McDowell, A., Nehrbass, D., Richards, R. G., & Moriarty, T. F. (2020). Longitudinal time-lapse in vivo micro-CT reveals differential patterns of peri-implant bone changes after subclinical bacterial infection in a rat model. *Sci Rep*, *10*(1), 20901. https://doi.org/10.1038/s41598-020-77770-z

Tamura, N., Ochi, M., Miyakawa, H., & Nakazawa, F. (2013). Analysis of bacterial flora associated with peri-implantitis using obligate anaerobic culture technique and 16S rDNA gene sequence. *Int J Oral Maxillofac Implants*, *28*(6), 1521-1529. https://doi.org/10.11607/jomi.2570

Thakur, A., Mikkelsen, H., & Jungersen, G. (2019). Intracellular Pathogens: Host Immunity and Microbial Persistence Strategies. *J Immunol Res*, *2019*, 1356540. https://doi.org/10.1155/2019/1356540

Wallis, J., Cho, S., & Diecidue, R. (2011). Propionibacterium Acnes: An Opportunistic Oral Pathogen. *Journal of Oral and Maxillofacial Surgery*, *69*(9), e5.

https://doi.org/10.1016/j.joms.2011.06.027

Werner, J. L., Escolero, S. G., Hewlett, J. T., Mak, T. N., Williams, B. P., Eishi, Y., & Núñez, G. (2017). Induction of Pulmonary Granuloma Formation by Propionibacterium acnes Is Regulated by MyD88 and Nox2. *Am J Respir Cell Mol Biol*, *56*(1), 121-130. https://doi.org/10.1165/rcmb.2016-0035OC

Abstract in Korean

치료에 반응하지 않는 구강 질환에서 세포 내 *Cutibacterium acnes* 균의 병리학적 역할

*Cutibacterium acnes (C. acnes)*는 피부 및 점막에 서식하는 혐기성 세균으로 정상세균총에 속하지만, 최근 다양한 만성 염증성 질환에서 병원균으로 작용할 수 있음이 밝혀지고 있다. 특히 대식세포 내에서 장기간 생존하는 특성은 면역 회피 및 만성 염증 유발과 관련이 있는 것으로 추정되나 세포 내 생존이 구강 염증성 질환에서 어떤 병리학적 역할을 하는지에 대한 연구는 미비하다.

본 연구에서는 치과 임플란트 주위염 및 근관 치료 후 치근단 병소로부터 세포 내 감염된 *C. acnes* 를 분리하여, 이 균주들이 세포 내 감염의 특징을 가지는 지에 대해 세포 실험 (in vitro) 및 생체 내 마우스 모델 (in vivo)를 통해 분석하였다.

그 결과, 분리된 *C. acnes* 균주는 Raw 264.7 대식세포주에서 10 일 이상 관찰이 되었으며, 일부 균주는 세포 내에서 사멸되지 않은 채 존재하는 것이 확인되었다. 세포 내 C. acnes 의 증식은 정량화 된 결과로 증명되지는 않았지만, 감염된 대식세포로부터 인접한 대식세포로의 전파 (intercellular propagation)가 형광 이미지 분석으로 확인되었다. 즉, 구강 염증성 질환 유래 *C. acnes* 가 대식세포에 지속적으로 존재하며 세포 간 확산이 가능함을 시사한다.

또한, *C. acnes* 의 감염은 대식세포에서 강한 염증성 사이토카인 반응을 유도하였다. 역전사 중합효소 연쇄 반응 (RT-PCR) 및 사이토카인 어레이 분석 결과 IL-6, CCL2, CSF2 와 같은 염증성 사이토카인 및 케모카인이 공통적으로 증가하였다. 전장 전사체 분석 (RNA sequencing)에서 *C. acnes* 의 감염은 1,672 개의 유전자의 발현 증가와 1,464 개의 감소가 확인되었으며, 증가된 유전자들은 주로 미생물 감염, 사이토카인 신호전달, 세포 내 감염에 대한 반응 들과 관련되었다.

마우스 피하 주입 실험에서 살아있는 *C. acnes* 를 주입한 부위에서 $CD68^{+}$ 대식세포 내에 장기간 잔존하고 있는 세균이 관찰되었으며, 육아종성 염증 반응이 유도되었다. 또한 염증 부위에서 IL-1β, IL-23, TNF-α 의 발현 증가가 관찰되었다.

열사멸된 세균에서도 염증 반응은 유도되었으나, 살아 있는 균을 주입했을 때 더 심한 괴사성 염증반응이 관찰되었다.

본 연구는 *C. acnes* 가 대식세포 내에서 생존하며 염증을 유발하는 세포 내 병원균으로 작용할 수 있음을 강하게 시사한다. 특히 치료에 반응하지 않는 구강 염증성 질환에서 *C. acnes* 의 세포 내 병원균으로서 특징이 치료 저항성 및 재발의 병리적 원인으로 작용할 수 있음을 시사한다. 나아가 기존 항생제나 치료 방식으로는 해결이 어려운 난치성 염증 병소에서 세포 내 감염균을 표적으로 하는 새로운 치료 전략의 필요성을 제시하고자 한다.

핵심되는 말 *: Cutibacterium acnes*, 대식세포, 세포 내 병원균, 염증, 감염, 임플란트주위염, 치근단 주위염, 구강 염증성 질환